Heikki Minn, MD[2] • Kenneth R. Zasadny, PhD • Leslie E. Quint, MD • Richard L. Wahl, MD

Lung Cancer: Reproducibility of Quantitative Measurements for Evaluating 2-[F-18]-Fluoro-2-deoxy-D-glucose Uptake at PET[1]

PURPOSE: **To study the precision of repeated 2-[fluorine-18]-fluoro-2-deoxy-D-glucose (FDG) uptake measurements at positron emission tomography (PET) in patients with primary lung cancer.**

MATERIALS AND METHODS: **Ten patients with untreated lung cancer underwent two dynamic FDG PET examinations after a 4-hour fast within 1 week. Kinetic modeling of tumor FDG uptake was performed on the basis of a three-compartment model. The tumor concentration of F-18 (standardized uptake value calculated on the basis of predicted lean body mass [SUV-lean]) was also measured 50–60 minutes after injection of a tracer. Blood glucose, insulin, and free fatty acid levels were monitored.**

RESULTS: **SUV-lean and the FDG influx constant K_i were measured with a mean ± standard deviation difference of 10% ± 7 and 10% ± 8, respectively, over repeated PET scans. The mean difference was reduced to 6% ± 6 and 6% ± 5 by multiplying SUV-lean and K_i by plasma glucose concentration.**

CONCLUSION: **SUV-lean and graphical K_i can be measured reproducibly, supporting their use in quantitative FDG PET algorithms.**

Index terms: Emission CT (ECT), 60.12163 • Fluorine • Glucose • Lung, emission CT (ECT), 60.12163 • Lung neoplasms, 60.321

Radiology 1995; 196:167–173

POSITRON emission tomography (PET) has the potential to improve the diagnosis, staging, and treatment monitoring of a variety of human tumors (1). Thoracic tumors represent a particular challenge for oncologists because they are not always readily accessible for tissue diagnosis without invasive procedures. PET imaging with 2-[fluorine-18]-fluoro-2-deoxy-D-glucose (FDG) or L-[methyl-carbon-11]-methionine has been shown to be useful for assessing solitary pulmonary nodules on the basis of the differential uptake in nonneoplastic and malignant lesions (2–6). Furthermore, the recent Radiologic Diagnostic Oncology Group trial showed the accuracies of computed tomography (CT) and magnetic resonance imaging to be comparably poor in the staging of mediastinal nodal metastases (about 50%–60%) (7). Their data indicated that FDG PET was significantly superior to CT in staging mediastinal tumors in patients with newly diagnosed lung cancer (8). Clearly, the use of PET to evaluate patients with lung cancer may eventually reduce the need for certain invasive or diagnostic procedures (9,10). Diagnostic algorithms based on the extent of FDG uptake have been proposed to fully implement PET as a diagnostic tool for the evaluation of solitary pulmonary opacities and mediastinal nodes (3,5,6,8).

The measurement of FDG uptake with PET provides an index of glucose metabolism in tumor, which, in turn, is used to assist in diagnostic workup and evaluation of treatment options. FDG uptake can be calculated with kinetic models that require measurement of tracer radioactivity input function by means of frequent blood sampling (11) or noninvasive measurement of radioactivity in the arterial blood pool (eg, from the left atrium [12] or aorta [13,14]). A simpler approach for the evaluation of FDG uptake in tumor is to measure tumor radioactivity concentration with normalization to the injected dose and total or lean body mass (11,15,16). In both kinetic and single-scan methods, patients are asked to fast to minimize unwanted elevations in blood glucose and insulin concentrations, which may affect the bioavailability of the tracer and, thus, tumor uptake (17,18). The standardization of the FDG PET imaging protocol is necessary not only for initial primary tumor and lymph node characterization but also for comparison with repeat scans once treatment has been started.

Unfortunately, the precision of these quantitative methods—even if carried out in fasted patients without intervening treatment—has not, to our knowledge, been carefully studied in patients with malignant tumors. It is not known how sensitive various quantitative measurements are to changes in host and tumor-related factors over a short time span when the effect of tumor growth on tracer uptake would be considered negligible. Consequently, quantitative FDG uptake studies in tumor tissue have generally been interpreted with caution by using reference to visual assessment of radionuclide accumula-

[1] From the Departments of Internal Medicine, Division of Nuclear Medicine (H.M., K.R.Z., R.L.W) and Radiology (L.E.Q.), University of Michigan Medical Center, 1500 E Medical Center Dr, B1G412, Ann Arbor, MI 48109-0028. Supported in part by National Cancer Institute grants CA 52880, CA53172, and CA56731; a grant from the Academy of Finland; and by the General Clinical Research Center at the University of Michigan (funded by grant M01RR00042 from the National Center for Research Resources, National Institutes of Health, U.S. Public Health Service). Received December 22, 1994; revision requested January 16, 1995; revision received February 22; accepted February 23. **Address reprint requests to** R.L.W.

[2] Current address: Department of Oncology and Radiotherapy, Turku University Central Hospital, Turku, Finland.

Abbreviations: FDG = 2-[fluorine-18]-fluoro-2-deoxy-D-glucose, FFA = free fatty acid, PET = positron emission tomography, ROI = region of interest, SD = standard deviation, SUV-lean = standardized uptake value calculated on the basis of predicted lean body mass.

tion, morphologic imaging methods, and clinical history (19,20). We carried out the current study in patients with newly diagnosed lung cancer to assess variability and reproducibility of both kinetic and single-scan methods for measurement of FDG uptake in tumor. The rationale was to provide a basis for the use of quantitative methods in further clinical trials assessing the accuracy of PET in lung cancer management but with the expectation that our results could be generalized to other forms of cancer.

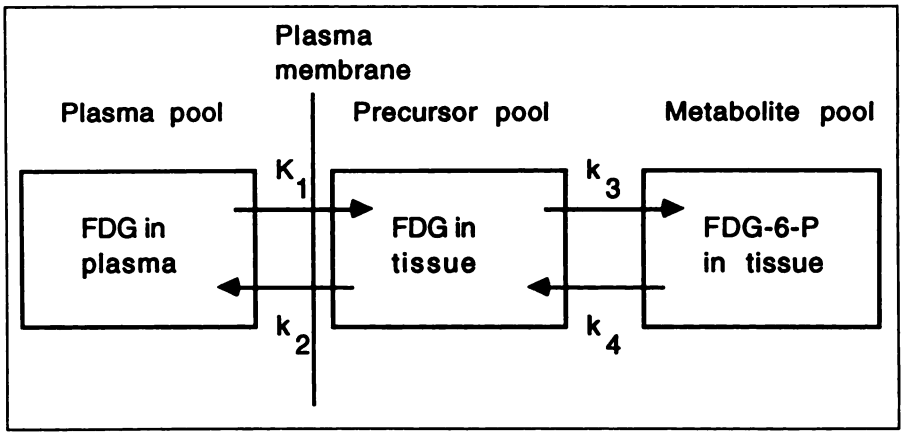

Figure 1. Three-compartment model for calculating the regional metabolic rate for glucose with FDG PET. The model assumes three compartments: free FDG in plasma, a precursor pool of unmetabolized FDG in tissue, and phosphorylated FDG (*FDG-6-P*) in tissue. The phosporylated FDG in the third compartment is not considered substrate for further forward metabolism. K_1, k_2, k_3, and k_4 are rate constants for FDG forward and reverse transport, phosphorylation, and dephosphorylation, respectively. (Adapted from reference 23.)

MATERIALS AND METHODS

Patient Population

Our study group consisted of 10 patients evaluated at the Thoracic Tumor Board between 1993 and 1994. All patients underwent routine diagnostic work-up including CT of the thorax and abdomen and pulmonary function tests. Patients were admitted to the study if they had a newly detected primary lung cancer or a lung nodule with a high suspicion of malignancy. We included only patients in whom the diameter of the primary lesion measured at least 2.0 cm in all three orthogonal dimensions (as measured from a CT scan) to avoid the need for correction of partial volume effects. None of the patients had known diabetes or was taking drugs known to affect glucose metabolism. One patient (patient 2) had undergone resection of the left upper lobe because of a stage I bronchogenic adenocarcinoma 1 year earlier, and one (patient 10) had undergone resection of the right lower lobe because of a reportedly limited ipsilateral small cell lung carcinoma 5½ years earlier. Both patients had received radiation therapy and patient 10 also received chemotherapy at the time of the previous diagnosis. None of the other patients was receiving any treatment for a malignant disease at the time of participating in the present study protocol.

The protocol was reviewed and approved by the Institutional Review Board of the University of Michigan. FDG was prepared under conditions of an Investigational New Drug Exemption accepted by the U.S. Food and Drug Administration. The nature of the study was explained orally to the patients before obtaining written informed consent. After completion of the current protocol, the diagnosis and tumor stage were confirmed at thoracotomy in all patients with non–small cell lung cancer (21). In contrast, two patients later shown to have a small cell carcinoma at fine-needle biopsy were subsequently referred to nonsurgical treatments.

Imaging Procedure

PET was performed in eight patients with an ECAT 921/EXACT scanner (CTI, Knoxville, Tenn, distributed by Siemens Medical Systems, Iselin, NJ); in two patients (patients 3 and 7), imaging was performed with an ECAT 931/08 scanner (CTI). The ECAT 921 scanner permits simultaneous acquisition of 47 transverse planes of 3.4-mm thickness encompassing a 15.0-cm axial field of view; the ECAT 931 scanner permits acquisition of 15 transverse planes with a 6.75-mm thickness and a 10.3-cm axial field of view. The patients fasted for at least 4 hours (except for ad libitum water) before undergoing PET. Two serial FDG PET examinations (denoted as study 1 and study 2) were performed in each patient within 1 week. At each examination, a catheter was placed in the antecubital vein opposite to the tumor and blood drawn prior to scanning to determine concentrations of plasma glucose, insulin, and free fatty acid (FFA). Brief transmission scanning (4–5 minutes) was performed with patients in the supine position and a ring source filled with germanium-68 and gallium-68. The transmission scan typically enabled the precise localization of the primary tumor and bronchial carina, which is essential for final determination of the level imaged to ensure that both tumor and areas of possible regional metastatic spread were included. The field of view was then marked with a felt pen on the skin by using a laser beam alignment system to enable accurate repositioning for the second study. Subsequently, a 12-minute transmission scan was obtained for photon attenuation correction used in the subsequent PET acquisition data reconstructions.

FDG was produced according to a standard nucleophilic fluorination method as previously described (22). A bolus of approximately 370 MBq of FDG was injected over 30 seconds by using the previously attached venous line. The mode of data acquisition was identical in sequential scans and consisted of six 10-second frames, three 20-second frames, two 90-second frames, one 300-second frame, and five 600-second frames. Finally, blood was again drawn to measure glucose and insulin levels at the conclusion of scanning.

Image Processing and Data Analysis

The average scanner efficiency rate for the study period was 156 cps/pixel/kBq/mL for the ECAT 921 scanner and 170 cps/pixel/kBq/mL for the ECAT 931 scanner. Cross-sectional sinogram data were corrected for dead time, decay, random coincidence, and attenuation. Image reconstruction was performed by means of a filtered back projection algorithm employing a Hanning filter with a cut-off frequency of 0.3 and a 128 × 128 matrix. The average x-y spatial resolution was 1.2 cm full width half maximum in plane for both and scanners. The last (50–60-minute) frame of the dynamic acquisition was used to define regions of interest (ROIs) for analysis of uptake of F-18 activity in tumor, which was invariably easily detectable as a "hot" area on a lower pulmonary tissue activity background. A computerized semiautomated algorithm was employed to eliminate interobserver discrepancy and to maximize interstudy reproducibility. This method helps define the maximal FDG uptake in a small square 1.2 × 1.2-cm ROI (4 × 4 pixels) placed within a large ROI covering the whole tumor and resulted in 100% agreement between two observers (H.M., K.R.Z). The ROIs over all planes covering tumor were reviewed, and counts were averaged in three (ECAT 921 scanner) or two (ECAT 931 scanner) contiguous sections with the highest activity. Standardized uptake values calculated on the basis of predicted lean body mass (SUV-lean) were determined in this maximal uptake ROI, as described previously (16). The same volume-averaged ROIs were also used in the kinetic analysis.

To define the input function needed for kinetic parameter estimation, blood time-

Table 1
Clinical and Histologic Findings in 10 Patients with Primary Lung Cancer

Patient No./Age (y)/Sex	Weight (kg)	Lean Body Mass (kg)*	Tumor Size (cm)†	Tumor Location	Histologic Finding	Tumor Stage‡
1/66/M	79	79	4 × 3 × 5	Left upper lobe	Adenocarcinoma	IIIA
2/82/M	70	67	5 × 5 × 7	Left upper lobe	Squamous cell carcinoma	IIIB
3/71/F	61	55	3 × 3 × 6	Right lower lobe	Squamous cell carcinoma	IIIA
4/61/M	75	59	3 × 4 × 4	Left hilum	Small cell carcinoma	Limited
5/69/M	75	73	4 × 3 × 4	Lingula	Small cell carcinoma	Limited
6/56/F	68	68	3 × 2 × 2	Right hilum	Squamous cell carcinoma	IIIA
7/58/F	63	55	7 × 9 × 8	Right upper lobe	Large cell carcinoma	IIIA
8/65/M	97	73	4 × 4 × 4	Right lower lobe	Squamous cell carcinoma	IIIA
9/49/M	76	67	4 × 5 × 4	Right upper lobe	Squamous cell carcinoma	IIIA
10/62/M	75	75	5 × 3 × 4	Right upper lobe	Squamous cell carcinoma	IIIA

* Lean body mass = weight in cases where estimated lean body mass was larger than true weight (15).
† Maximum extent in three orthogonal dimensions as determined from CT scan.
‡ Determined surgically in non–small cell cancer and clinically in small cell carcinoma. Stage is given according to guidelines of the American Joint Committee on Cancer (20).

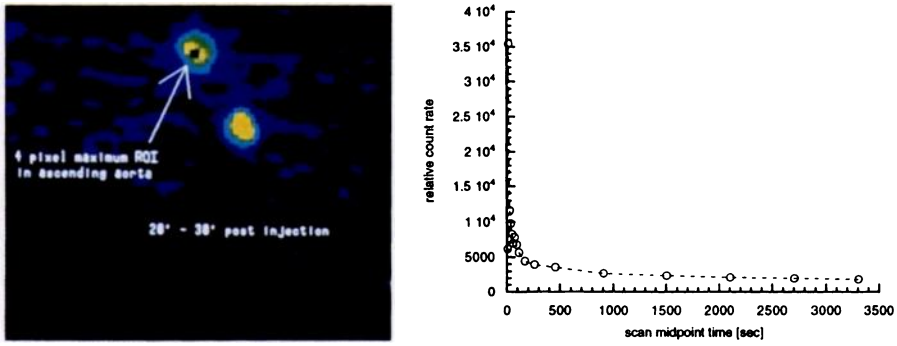

a. b.

Figure 2. **(a)** PET scan shows determination of the ROI from the ascending aorta (arrow) at the level of the bronchial carina for noninvasive measurement of arterial input function of radioactivity. The descending aorta is also well delineated. **(b)** Representative time-activity curve derived from the ascending aorta.

activity curves were generated by centering a 4-pixel ROI in the ascending aorta at the level of the carina and a 16-pixel ROI in the left atrium (12–14). Typically, the second or third frame of the dynamic study was used for ROI definition, and the maximal counts per pixel within the aorta were averaged over three contiguous planes. For the left atrium, only one plane was used. The mean diameter of the ascending aorta (measured at the level of the carina on the CT scan obtained 1–14 days before PET) was 3.3 cm (range, 2.8–3.9 cm).

A standard three-compartment metabolic model (Fig 1) was used to quantitatively assess kinetics of FDG transport and phosphorylation in tumor tissue (23). The formalism of the model generates kinetic parameters (ie, transfer rate constants for FDG transport from blood to tissue [K_1], return of the unmetabolized tracer to plasma pool [k_2], and intracellular phosphorylation of FDG to FDG-6-phosphate [k_3]). Because the rate of conversion of FDG-6-phosphate to FDG was empirically found to be negligible compared with $K_1 - k_3$ in the first three patients of the present study and in our previous study of breast tumor kinetic modeling (12), the rate of dephosphorylation (k_4) was assumed to be zero in further analysis.

The kinetic model produces an estimate of the net rate of FDG phosphorylation in tumor (K_c), as follows: $K_c = (K_1 \cdot k_3)/(k_2 + k_3)$. K_c is equal to the influx constant K_i, which is determined from a graphical analysis of unidirectional FDG influx as defined by Patlak et al (24). By multiplying Kc or K_i by the average plasma glucose concentration during PET scanning, the metabolic rate of FDG in tumor can be obtained (11). This index is considered to reflect tumor use of glucose, although absolute values for glucose metabolism cannot be estimated with certainty due to the variable differences in the affinities of FDG and glucose for transport and phosphorylation in generally heterogenous malignant tissue (25).

Statistical Analysis

The reproducibility of blood curves was assessed by comparing the differences in areas under the dynamic time-activity curves corrected for injected dose in studies 1 and 2. The differences in individual quantitative parameters between the two studies were compared with the pairwise Student t test. To assess the intrasubject variability of all parameters, mean percentage differences were calculated with the following formula:

$$\sum_{i=1}^{10} \frac{|X_{i1} - X_{i2}|}{\overline{X}_i},$$

where X_{i1} is the parameter value in study 1, X_{i2} the corresponding value in study 2, and $\overline{X}_i$ the mean of X_{i1} and X_{i2}. To assess the reproducibility of each parameter, standard deviations (SDs), confidence intervals, and reliability coefficients were determined. The reliability coefficient measures intraclass correlation (ie, the correlation between two measurements observed in the same individual at different times) (26,27). Briefly, one-way analysis of variances using patients as independent variables were computed for determination of intraclass correlation coefficients. The correlation coefficient was obtained from the F statistics of the analysis of variance, as follows: $r = (F - 1)/(F + n - 1)$, where n is the number of measurements for each subject. All P values are two-tailed.

RESULTS

A summary of the patient characteristics is shown in Table 1. Figure 2 shows the ROI selection and the time-activity curve obtained from the ascending aorta. Figure 3 shows a representative example of sequential thoracic FDG PET scans obtained in patient 3. Table 2 shows individual tumor-related quantitative parameters and concentrations of plasma glucose, insulin, and FFA. Table 3 shows the mean ± SD for each of the measured parameters from studies 1 and 2. The difference between the parameters for the two studies was not statistically significant, although borderline significance was suggested for difference in FFA concentration ($P = .072$).

The reproducibility of blood curves obtained from the ascending aorta was better than that of curves obtained in the left atrium in terms of both the mean ± SD of the percentage difference of areas under the curve (9% ± 6 and 12% ± 8, respectively) and reliability coefficients (.942 vs .813). The interobserver variability in defining blood curves from the ascending aorta showed a mean percentage difference of only 3% in area under the curve defined from 14 scans of seven patients. Because further kinetic analyses of FDG uptake showed invariably better reproducibility of parameters obtained from the aorta rather than the left atrium, only the former are reported here.

Figure 4 shows individual inter-study differences of FDG uptake pa-

rameters in all patients. The SUV-lean and graphical analysis–derived FDG influx values (K_i) showed high reproducibility, as indicated by their low mean ± SD percentage differences of 10% ± 7 and 10% ± 8, respectively, and high reliability coefficients (0.987 and 0.969, respectively) (Table 4). SUV-lean and K_i had a strong correlation ($r^2 = .92$, $P < .001$; Fig 5) in all 20 FDG PET studies performed. By multiplying the FDG uptake index with the mean plasma glucose concentration, a tendency toward further reduction in the difference was obtained for both SUV-lean and K_i—to 6% ± 6 ($P = .058$) and 6% ± 5 ($P = .265$), respectively. This was also true for the kinetic model–derived influx constant (K_c), which showed slightly higher variabilities of 16% ± 12 (baseline) and 11% ± 11 (glucose corrected, $P = .075$) than SUV-lean and K_i. K_c was always greater than K_i ($P < .001$).

The individual rate constants ($K_1 - k_3$) had notably higher between-study variability, as evidenced by their mean differences of 24% ± 15, 42% ± 31, and 24% ± 13, respectively. The rate constant for intracellular FDG phosphorylation (k_3) still had a high reliability coefficient of 0.953. The sensitivity of graphical analysis and model-derived parameters for interobserver variability or the use of an alternate fit starting point in a single study was studied separately (Table 5). Of all quantitative tracer-uptake parameters studied, that depicting FDG efflux from the intracellular compartment (k_2) again showed the highest variability in terms of all modes of statistical evaluation.

The absolute difference in glucose and insulin concentrations between studies 1 and 2 was not statistically significant, showing that none of the patients had abnormally high fasting values suggestive of impaired glucose tolerance. The somewhat higher variability in FFA concentrations was not reflected in parallel changes of tumor FDG uptake. Of these three factors illustrating patient metabolic state during PET, only glucose concentration appeared to be associated with tumor uptake of FDG.

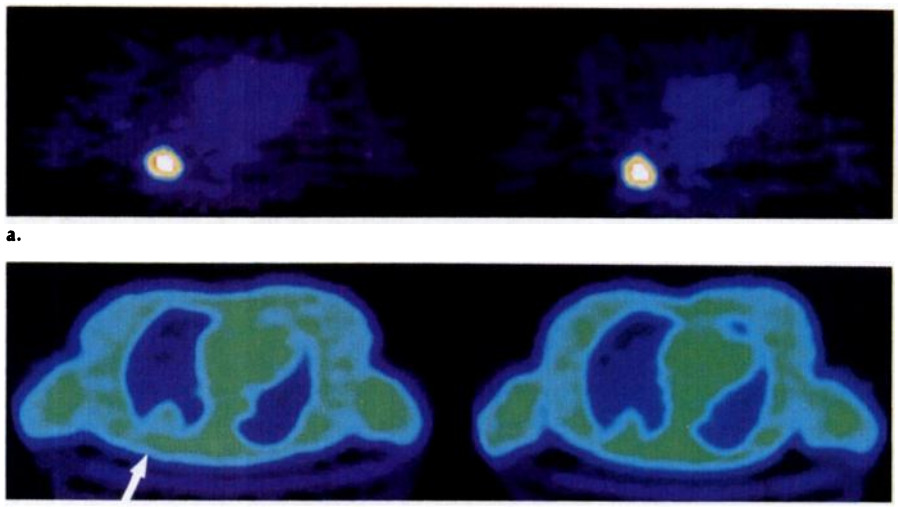

Figure 3. Thoracic **(a)** emission and **(b)** transmission PET scans of a patient with a right lower lobe primary squamous cell carcinoma (patient 3). Both emission scans, obtained on consecutive days in the fasting state, show intense FDG uptake in tumor. The SUV-lean was 8.6 in study 1 and 8.7 in study 2. Note that the tumor is easily visualized as an opacity in the right posterior lung on the transmission scan (arrow in **b**).

DISCUSSION

The current study was designed to investigate the precision at which various measurements of FDG uptake could be assessed in patients with potentially resectable lung cancer. The study is a part of a larger protocol evaluating the utility of PET in presurgical staging of non–small cell lung cancer. We studied clinically nondiabetic patients in the fasting state twice within 1 week to minimize tumor-growth and patient-related factors known to increase the variability of FDG uptake measurements. Indeed, we detected normal fasting glucose and insulin concentrations on sequential PET scans where slight changes of 8% and 20% probably indicated differences in times since last meal rather than subclinical diabetic disease. The larger mean difference of 29% in plasma FFA concentration may be in accordance with slower clearance of fatty acid residues after food ingestion and length of fast before PET (28). The effect of the blood fatty acid pool on FDG uptake in tumor is poorly understood, although it is assumed to be small because of the low use of fatty acids in comparison to glucose seen in preclinical studies (29,30).

We found that SUV-lean, graphical K_i, and, to a lesser extent, model-derived influx constant K_c showed only modest variability, which could be further reduced by multiplying the FDG uptake index by mean glucose concentration. On the basis of our initial data, a change in SUV-lean or K_i of more than 25% that corresponds to a change of mean variability ± two SDs would be suggestive of a true increase or decrease in tumor glucose metabolism caused by, for example, radiation or chemotherapy. Conversely, a change in k_3 of more than 50% is required to be certain that the observed difference is due to treatment-related variance. These observations were made in a series of lung tumors of at least 2 cm in diameter in all three orthogonal dimensions to overcome problems associated with partial volume effects and repositioning errors. One may speculate that larger variability is possible in very small lesions where decreased count recovery and possible positional differences on serial scans may have a proportionately larger effect.

Although, to our knowledge, the usefulness of quantitative evaluation of cancer treatment with PET has not been conclusively shown (31), the initial experience in breast (12) and head and neck cancer (32) has been promising. We thus would advocate the use of simple methods of quantitation like SUV-lean and graphical K_i because they are less sensitive than compartmental analysis to slight differences during data acquisition and reconstruction and thus more reproducible. The noninvasive method for determination of the blood input curve from the left atrium or aorta is feasible in thoracic tumors but necessitates dynamic scanning from the outset of the study. However, the constraints of the selection of the proper time-point for steady-state evaluation can be avoided (33). This is a concern after treatment and may affect phosphorylation and transport of FDG in an unpredictable way and change the temporal pattern of FDG uptake. Another concern is how to implement partial volume correction in serial studies of small lesions. Because of the irregular shape and often poor demarcation of shrinking tumors, their size may not be easily defined on morphologic images.

Table 2
Summary of Sequential Quantitative PET Parameters in 10 Patients with Lung Cancer

Patient No.	Study No.	Glucose Level (mmol/L)	Insulin Level (pmol/L)	FFA Level (mEq/L)	SUV-lean*	K_i	K_c	K_1	k_2	k_3	Interval between Studies (d)
1	1	5.7	66	0.48	16.4	0.0777	0.0813	0.242	0.454	0.230	2
	2	6.3	65	0.50	14.7	0.0841	0.0979	0.191	0.160	0.168	
2	1	7.6	102	0.68	6.3	0.0345	0.0349	0.102	0.552	0.287	1
	2	7.2	54	1.82	6.1	0.0351	0.0396	0.146	0.607	0.225	
3	1	5.5	63	1.12	8.6	0.0441	0.0525	0.135	0.264	0.169	1
	2	5.4	45	1.47	8.7	0.0514	0.0558	0.178	0.550	0.250	
4	1	5.8	143	0.83	7.7	0.0432	0.0504	0.117	0.186	0.141	1
	2	5.4	147	0.9	8.0	0.0458	0.0534	0.112	0.094	0.087	
5	1	5.9	147	0.88	9.3	0.0521	0.0571	0.080	0.022	0.054	1
	2	6.7	132	1.03	7.6	0.0442	0.0473	0.065	0.018	0.049	
6	1	5.5	32	0.99	3.4	0.0159	0.0252	0.100	0.219	0.074	1
	2	5.6	44	1.29	2.9	0.0163	0.0201	0.122	0.294	0.058	
7	1	4.9	125	1.03	12.4	0.0716	0.0820	0.133	0.044	0.070	1
	2	5.7	146	0.83	10.6	0.0591	0.0679	0.115	0.056	0.081	
8	1	5.8	158	0.31	4.6	0.0335	0.0340	0.049	0.180	0.406	7
	2	6.1	201	0.59	4.3	0.0332	0.0326	0.049	0.162	0.319	
9	1	5.1	164	0.54	6.9	0.0323	0.0393	0.188	0.267	0.070	1
	2	5.3	174	0.57	7.7	0.0337	0.0420	0.123	0.127	0.066	
10	1	5.4	122	0.48	7.4	0.0365	0.0489	0.105	0.096	0.084	2
	2	6.2	137	0.65	6.6	0.0295	0.0311	0.064	0.070	0.068	

* SUV-lean is a dimensionless parameter. The unit for all the kinetic FDG uptake parameters is $1 \cdot min^{-1}$.

Table 3
Quantitative Parameters in Sequential FDG-PET Studies of 10 Patients with Lung Cancer

Parameter	Study 1	Study 2
Glucose (mmol/L)	5.7 ± 0.7	5.9 ± 0.6
Insulin (pmol/L)	112 ± 45	115 ± 57
FFA (mEq/L)	0.73 ± 0.28	0.97 ± 0.44
SUV-lean	8.3 ± 3.8	7.7 ± 3.3
K_i	0.044 ± 0.019	0.043 ± 0.019
K_c	0.051 ± 0.019	0.049 ± 0.022
K_1	0.125 ± 0.055	0.117 ± 0.047
k_2	0.228 ± 0.169	0.214 ± 0.207
k_3	0.159 ± 0.117	0.137 ± 0.097

Note.—None of the differences between the two studies were statistically significant. Data are given as mean ± SD.

Finally, the influence of inflammatory cells and fibroblasts within residual tumor could be confusing after treatment (15,34).

As expected, there was a wide range of individual rate constants (24%–42%), which reflects the difficulty of applying a rather simple three-compartment model to quantitate metabolism in a heterogenous tissuelike tumor. Nevertheless, similar observations have been characteristically seen in noncancerous tissues as well, showing that more robust numeric indexes of the net phosphorylation rate of FDG (K_i and K_c) are less sensitive to errors due to the correlation between the individual rate constants in the fitting process (35). Because the errors in estimating microparameters tend to cancel each other out, measurements of the total FDG metabolic rate graphically or by calculating from individual rate constants will consistently lead to a smaller variability (36).

The use of the ascending aorta instead of the left atrium to noninvasively obtain the blood input curve was found consistently to yield more reproducible measurements, as confirmed by the excellent match of curves defined independently by the two observers. In line with this, less variability was found for kinetic fits of FDG uptake when the aorta instead of the left atrium was used to measure blood radioactivity. Indeed, the fairly good reproducibility of the sequential aortic input curves (mean percentage difference of 9% in area under the curve measurements) suggests that differences in the blood radioactivity measurements are not responsible for the observed variability in k_3, K_c, and K_i, that is, the variability of parameters that depict FDG accumulation rather than instantaneous uptake and reverse transport. As discussed by Lammertsma et al (34), differences in the FDG injection technique may affect the precision of rate constant measurements and probably affect more greatly those related to transport (K_1 and k_2) than K_c and K_i. However, even when interobserver evaluation of the same tissue and blood data sets was performed by experienced observers, a variability of 4%–34% was detected. This supports inherent limitations and discrepancies in interpretation of model-related dynamic acquisition data fitting.

The increasing demand for clinical applications of PET imaging in patients with cancer has not resulted in a consensus over how increased uptake of FDG in tumors should be assessed. The rationale for quantitative imaging is reflected in the difficulties of pure visual and morphologic tumor characterization and a need for accurate assessment of treatment effects. There has been a general concern about whether quantitation of glucose metabolism in tumors is feasible with FDG PET owing to the heterogenous nature of malignant tissue even in tumors of the same histologic and pathologic grade (25). The very limited knowledge about the so-called lump constant values in neoplastic tissues, which depict the differential affinities of FDG and glucose for transport and phosphorylation (23), indicate twofold regional differences in a single experimental tumor system for lump constants (37). It is doubtlessly safer not to translate FDG uptake rates in tumors to measures of glucose use, although phosphorylation of FDG, once transported to tumor cells, obviously reflects aerobic and anaerobic glycolysis, which is a major form of energy metabolism in cancer (38).

The controversy in defining absolute values of glucose use in tumors has resulted in the development of simpler means for quantitation of FDG uptake (eg, SUV-lean). Even when employing these generally acceptable and useful methods, it must

be realized that many temporally changeable factors (eg, blood glucose and insulin levels and general patient nutritive status) strongly affect FDG uptake and must be controlled if quantitation is the goal of the PET study. Hyperglycemia and hyperinsulinemia, which are common in diabetic and malnourished cancer patients, result in delayed clearance of FDG from blood or shift tracer uptake to insulin-sensitive tissues (eg, muscles) (17,39). Although fatty acids do not generally interfere with glucose uptake of insulin-insensitive tissues like tumor (29,39), they may affect the appearance of FDG PET signal by competitive inhibition with glucose in, for example, adjacent muscles (28). Effect of patient nutrition is also reflected in the proportions of various tissue compartments of which body fat is considered to be devoid of FDG accumulation (11,16). This has led to definition of less weight-dependent parameters where SUV is corrected for lean body mass (16) or body surface area (11,40).

The commonly adopted SUV formalism is confined to the measurement of radioactivity concentration at a fixed time point, leading to criticism of what would be the most appropriate time for assessment of tumor metabolism and comparison of biologic behavior of cancer between different patients (41). Hamberg et al (33) measured FDG uptake in eight lung tumors over 90 minutes and extrapolated time to reach a plateau tracer concentration on the basis of FDG kinetic model–derived estimations of progressive increase in dose uptake ratio, which is identical to SUV. In all cases, they found steadily increasing dose uptake ratios after a "conventional" imaging time of 60 minutes and predicted the average time to reach 95% of the plateau dose uptake ratio to be 298 minutes ± 42 in the pretreatment phase. They concluded that the true malignant nature of lung tumors may be overlooked in a single static acquisition. Although it may be inconvenient to determine the plateau phase of FDG uptake kinetics, it is relatively easy to measure the rate of accumulation (K_i, K_c), which is constant over standard acquisition times. However, results of our study and a larger series of FDG PET in 46 patients with head and neck cancer and lymphoma (r^2 = .83 for K_i multiplied by glucose vs SUV and r^2 = .88 vs SUV corrected for body surface area) (11) indicate a very strong correlation between kinetic and SUV evaluation 50–60 minutes after injection. Similar strong correlations have been seen between SUV and K_i in patients with breast cancer (12). These observations and precision speak in favor of a single-scan approach for diagnostic purposes, and we believe that it is a precise method for evaluating solitary pulmonary nodules (3,5,6,8). A possible exception is an insulin-resistant diabetic state that has not been controlled with adequate dietary and pharmacologic measures (11).

Although treatment effects on kinetic parameters have been successfully evaluated in breast and liver tumors (12,42), the widespread use of kinetic analysis in lung cancer outside research protocols is not supported by the current study. Rather, the substantial variability in $K_1 - k_3$ suggests they may be much more challenging to apply in treatment monitoring to individual patients than simple parameters like SUV-lean or K_i. However, the usefulness of these parameters should be assessed in trials that address a treatment effect on a specific step of FDG metabolism (eg,

Table 4
Variability of Quantitative Parameters between Studies 1 and 2

Parameter	Percentage Difference*	Reliability Coefficient	95% Confidence Interval (%)	*P* Value
Glucose	8 ± 5	.844	5, 11	.009
Insulin	20 ± 19	.949	8, 32	<.003
FFA	29 ± 28	.603	12, 46	.080
Area under the curve				
Ascending aorta	9 ± 6	.942	5, 13	<.001
Left atrium	12 ± 8	.813	7, 17	.014
SUV-lean	10 ± 7	.987	6, 14	<.001
K_i	10 ± 8	.969	5, 15	<.001
K_c	16 ± 12	.935	9, 23	<.001
SUV-lean†	6 ± 6	.995	2, 10	<.001
K_i†	6 ± 5	.987	3, 9	<.001
K_c†	11 ± 11	.968	4, 18	<.001
K_1	24 ± 15	.812	14, 34	.015
k_2	42 ± 31	.765	23, 61	.025
k_3	24 ± 13	.953	16, 32	<.001

* Data are given as mean ± standard deviation.
† Glucose corrected.

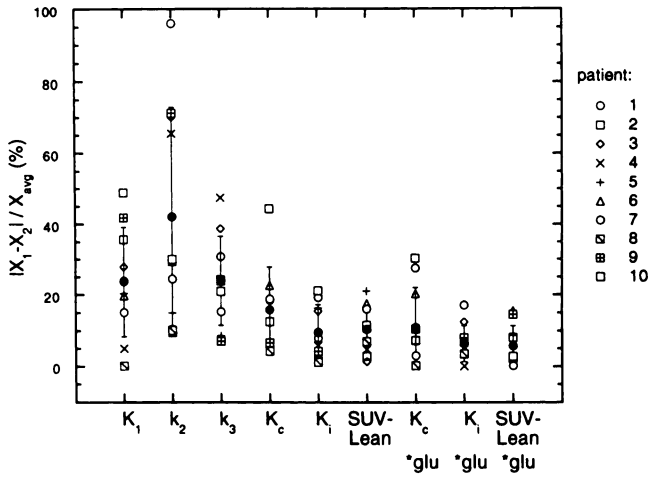

Figure 4. Variability of FDG uptake parameters of sequential PET scans in primary lung cancer. Mean percentage differences (•) are shown for all patients, suggesting improved reproducibility with correction of quantitative uptake indexes with plasma glucose concentration (*glu).

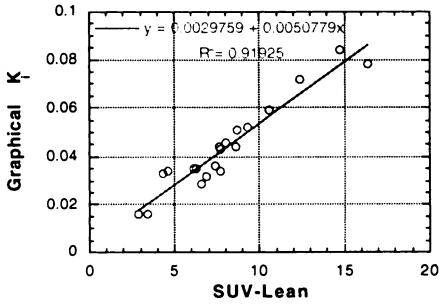

Figure 5. Relationship between SUV-lean and K_i in 20 FDG PET scans obtained in 10 patients with lung cancer.

Table 5
Sensitivity of FDG Uptake Parameters on Interobserver Analysis ($n = 7$) and Kinetic Model Fit Starting Point ($n = 10$) in One PET Study

Parameter	Interobserver Mean Percentage Difference	Reliability Coefficient	95% Confidence Interval (%)	Mean Percentage Difference of Alternate Fit Parameters	Reliability Coefficient	95% Confidence Interval (%)
SUV-lean	0	1.000	NA	NA	NA	NA
K_i	4	0.993	1, 7	0	1.000	0, 0
K_c*	5	0.978	1, 9	0	1.000	0, 0
K_1	11	0.957	1, 21	5	0.971	0, 13
k_2	34	0.910	0, 71	10	0.932	0, 25
k_3	22	0.914	1, 42	3	0.991	0, 8

Note.—NA = not applicable.
* Glucose corrected.

transport, which may be affected by increasing levels of hypoxia) (43). In the evaluation of indeterminate lung tumors, the use of modeling does not appear justified and indeed may be misleading.

In summary, we showed that both the single-scan approach with calculation of SUV-lean and a dynamic method where the FDG influx constant is determined graphically (K_i) provide highly reproducible indexes of glucose metabolism. Correction for plasma glucose concentration may further enhance precision of SUV-lean and K_i measurements. Estimates of microrate constants ($k_1 - k_3$) obtained from a three-compartment model to assess FDG transport and metabolism are much less precise in individual patients and should be used with caution. We advocate using simple methods of quantitating glucose metabolism in tumor for imaging lung cancer with FDG PET, making the initial diagnosis, and monitoring therapy. ■

Acknowledgments: The authors thank Sharon Fox, RN, and Peter Scheid, BA, for their contribution in patient accrual and scheduling. Morton S. Brown, PhD, is gratefully acknowledged for statistical advice and Brant Strand, BA, for help in data analysis. The technologists at the PET Suite and the staff at the Radiochemistry Laboratory are thanked for their skillful assistance.

References

1. Wahl RL. Positron emission tomography: applications in oncology. In: Murray IPC, Ell PJ, eds. Nuclear medicine in clinical diagnosis and treatment. Vol 2. New York, NY: Churchill Livingstone, 1994; 801–820.
2. Kubota K, Matsuzawa T, Fujiwara T, et al. Differential diagnosis of lung tumor with positron emission tomography: a prospective study. J Nucl Med 1990; 31:1927–1933.
3. Gupta NC, Frank AR, Dewan NA, et al. Solitary pulmonary nodules: detection of malignancy with PET with 2-[F-18]-fluoro-2-deoxy-D-glucose. Radiology 1992; 184:441–444.
4. Knopp MV, Bischoff H, Oberdorfer F, van Kaick G. Positronenemissionstomographie des thorax. Radiologe 1992; 32:290–295.
5. Patz EF, Lowe VJ, Hoffman JM, et al. Focal pulmonary abnormalities: evaluation with F-18 fluorodeoxyglucose PET scanning. Radiology 1993; 188:487–490.
6. Lowe VJ, Hoffman JM, DeLong DM, Patz EF Jr, Coleman RE. Semiquantitative and visual analysis of FDG-PET images in pulmonary abnormalities. J Nucl Med 1994; 35:1771–1776.
7. Webb WR, Gatsonis C, Zerhouni EA, et al. CT and MR imaging in staging non–small cell bronchogenic carcinoma: report of the Radiological Diagnostic Oncology Group. Radiology 1991; 178:705–713.
8. Wahl R, Quint L, Greenough R, Meyer C, White R, Orringer M. Staging of mediastinal non–small cell lung cancer with FDG PET, CT, and fusion images: preliminary prospective evaluation. Radiology 1994; 191:371–377.
9. Karsell PR, McDougall JC. Diagnostic tests for lung cancer. Mayo Clin Proc 1993; 68:288–296.
10. Mountain CF. Surgery for stage IIIa-N2 non–small-cell lung cancer. Cancer 1994; 73:2589–2598.
11. Minn H, Leskinen-Kallio S, Lindholm P, et al. [^{18}F]Fluorodeoxyglucose uptake in tumors: kinetic vs. steady-state methods with reference to plasma insulin. J Comput Assist Tomogr 1993; 17:115–123.
12. Wahl RL, Zasadny K, Helvie M, Hutchins GD, Weber B, Cody R. Metabolic monitoring of breast cancer chemohormonotherapy using positron emission tomography: initial evaluation. J Clin Oncol 1993; 11:2101–2111.
13. Dhawan V, Takikawa S, Robeson W, et al. Quantitative brain FDG/PET studies using dynamic aortic imaging. Phys Med Biol 1994; 39:1475–1487.
14. Ohtake T, Kosaka N, Watanabe T, et al. Noninvasive method to obtain input function for measuring tissue glucose utilization of thoracic and abdominal organs. J Nucl Med 1991;32: 1432–1438.
15. Haberkorn U, Strauss LG, Dimitrakapoulou, et al. PET studies of fluorodeoxyglucose metabolism in patients with recurrent colorectal tumors receiving radiotherapy. J Nucl Med 1991;, 32:1485–1490.
16. Zasadny K, Wahl RL. Standardized uptake values of normal tissues at PET with 2-[fluorine-18]-fluoro-2-deoxy-D-glucose: variations with body weight and a method for correction. Radiology 1993; 189:847–850.
17. Lindholm P, Minn H, Leskinen-Kallio S, Bergman J, Ruotsalainen U, Joensuu H. Influence of the blood glucose concentration on FDG uptake in cancer: a PET study. J Nucl Med 1993; 34:1–6.
18. Langen KJ, Braun U, Rota Kops E, et al. The influence of plasma glucose levels on fluorine-18-fluorodeoxyglucose uptake in bronchial carcinomas. J Nucl Med 1993; 34:355–359.
19. Wahl R, Quint L, Cieslak R, Aisen A, Koeppe R, Meyer C. "Anatometabolic" tumor imaging: fusion of FDG PET with CT or MRI to localize foci of increased activity. J Nucl Med 1993; 34:1190–1197.
20. Adler LP, Crowe JP, Al-Kaisi NK, Sunshine JL. Evaluation of breast masses and axillary lymph nodes with [F-18]2-deoxy-2-fluoro-D-glucose PET. Radiology 1993; 187:743–750.
21. Patel AM, Dunn WF, Trastek VF. Symposium on intrathoracic neoplasms. IV. Staging systems of lung cancer. Mayo Clin Proc 1993; 68: 475–482.
22. Toorongian SA, Mulholland GK, Jewett DM, Bachelor MA, Kilbourn MR. Routine production of 2-deoxy-2[18F]fluoro-D-glucose by nucleophilic exchange on a quaternary 4-aminopyridium resin. Int J Rad Appl Instrum [B] 1990; 17:273–279.
23. Phelps ME, Huang SC, Hoffman EJ, et al. Tomographic measurement of local cerebral glucose metabolic rate in human with (F-18)2-fluoro-2-deoxy-D-glucose: validation of method. Ann Neurol 1979; 6:371–388.
24. Patlak CS, Blasberg RG, Fenstermacher JD. Graphical evaluation of blood-to-brain-transfer constants from multiple time uptake data. J Cereb Blood Flow Metab 1983; 5:179–192.
25. Graham MM, Lewellen TK. Positron emission tomography and its role in metabolic imaging (editorial). Mayo Clin Proc 1989; 64:725–727.
26. Scheffé H. The analysis of variance. New York, NY: Wiley, 1959; 221–260.
27. Vingerhoets FJG, Snow BJ, Schulzer M, et al. Reproducibility of fluorine-18-6-fluorodopa positron emission tomography in normal human subjects. J Nucl Med 1994; 35:18–24.
28. Ferrannini E, Barrett EJ, Bevilacqua S, DeFronzo RA. Effect of fatty acids on glucose production and utilization in man. J Clin Invest 1983; 72:1737–1747.
29. Cederbaum AI, Rubin E. Fatty acid oxidation, substrate shuttles, and activity of the citric acid cycle in hepatocellular carcinomas of varying differentiation. Cancer Res 1976; 36:2980–2987.
30. Mulligan HD, Beck SA, Tisdale MJ. Lipid metabolism in cancer cachexia. Br J Cancer 1992; 66:57–61.
31. Minn H, Paul R. Cancer treatment monitoring with fluorine-18 2-fluoro-2-deoxy-D-glucose and positron emission tomography: frustration or future (editorial). Eur J Nucl Med 1992; 19:921–924.
32. Lindholm P, Leskinen-Kallio S, Grénman R, et al. Evaluation of response to radiotherapy in head and neck cancer by positron emission tomography and [11C]methionine. Int J Radiat Oncol Biol Phys (in press).
33. Hamberg LM, Hunter GJ, Alpert NM, Choi NC, Babich JW, Fischman AJ. The dose uptake ratio as an index of glucose metabolism: useful parameter or oversimplification? J Nucl Med 1994; 35:1308–1312.
34. Lammertsma AA, Brooks DJ, Frackowiak RSJ, et al. Measurement of glucose utilisation with [^{18}F]2-fluoro-2-deoxy-D-glucose: a comparison of different analytical methods. J Cereb Blood Flow Metab 1987; 7:161–172.
35. Evans AC, Diksic M, Yamamoto YL, et al. Effect of vascular activity in the determination of rate constants for the uptake of 18F-labeled 2-fluoro-2-deoxy-D-glucose: error analysis and normal values in older subjects. J Cereb Blood Flow Metab 1986; 6:724–738.
36. Kubota R, Kubota K, Yamada S, Tada M, Ido T, Tamahashi N. Microautoradiographic study for the differentiation of intratumoral macrophages, granulation tissues and cancer cells by the dynamics of fluorine-18-fluorodeoxyglucose uptake. J Nucl Med 1994; 35:104–112.
37. Kapoor RR, Spence AM, Muzi M, Graham MM, Abbott GL, Krohn KA. Determination of the deoxyglucose and glucose phosphorylation ratio and the lump constant in rat brain and transplantable rat glioma. J Neurochem 1989; 53:37–44.
38. Eigenbrodt E, Fister P, Reinacher M. New perspectives on carbohydrate metabolism in tumor cells. In: Breitner R, ed. Regulation of carbohydrate metabolism. Vol 2. Boca Raton, Fla: CRC Press, 1985; 141–179.
39. Minn H, Nuutila P, Lindholm P, et al. In vivo effects of insulin on tumor and skeletal muscle glucose metabolism in patients with lymphoma. Cancer 1994; 73:1490–1498.
40. Kim CK, Gupta NC, Chandramouli B, Alavi A. Standardized uptake values of FDG: body surface correction is preferable to body weight correction. J Nucl Med 1994; 35:164–167.
41. Fischman AJ, Alpert NM. FDG-PET in oncology: there's more to it than looking at pictures (editorial). J Nucl Med 1993; 34: 6–11.
42. Okazumi S, Isono K, Enomoto K, et al. Evaluation of liver tumors using fluorine-18-fluorodeoxyglucose PET: characterization of tumor and assessment of effect of treatment. J Nucl Med 1992; 33:333–339.
43. Clavo AC, Brown RS, Wahl RL. 2-fluoro-2-deoxy-D-glucose (FDG) uptake into human cancer cell lines is increased by hypoxia. J Nucl Med (in press).